Spacecraft Design for Multipurpose Solar Electric Propulsion Missions

J. H. MOLITOR,* L. SCHWAIGER,† AND D. MACPHERSON‡
Hughes Aircraft Company, El Segundo, Calif.

The potential performance advantages of solar electric propulsion have led to a study of the over-all spacecraft systems implications of such propulsion devices. The results of this study, including spacecraft design and trajectory analysis (using the Atlas/Centaur as the launch vehicle) for asteroid belt, out-of-ecliptic, and solar probes are presented. These design studies have investigated the feasibility of a baseline spacecraft that could accommodate the requirements and constraints of each mission considered and indicate the degree of subsystem flexibility required of such a multipurpose spacecraft. Particular attention is devoted to a modular-ion engine system design that can perform a variety of missions with no basic modifications to major elements. A fixed attitude spacecraft design able to perform efficiently the three selected missions is described.

Introduction

A STUDY was performed to determine the feasibility and applicability of a single solar electric spacecraft (SEP) design for use in a variety of interplanetary space missions currently of interest to NASA. The major study tasks included trajectory and mission analyses, electric propulsion system design, and spacecraft design.

The three missions to be considered in detail were an asteroid belt probe, a solar probe, and an out-of-ecliptic probe (see Fig. 1). Although the asteroid belt probe was to be considered as the primary mission, off-optimum designs were to be explored as a compromise to make the spacecraft applicable to other missions. Although the electric propulsion system was modularized (making it flexible in terms of the number of thruster and power conditioning modules to be employed), an attempt was made to use the identical system for all missions. The launch vehicle that was chosen was the Atlas (SLV-3C)/Centaur with a standard OAO shroud.

The possibility of using the same basic spacecraft to perform more than one mission has often been raised because of its obvious attractions. The mission analysis in this paper differs from a previous proposal[1] in that the use of a slightly larger launch vehicle permits utilization of mission profiles that are much more compatible with practical mission time and reliability considerations.

An additional ground rule of the study was to attempt to employ hardware (especially in the case of the electric propulsion system) that is presently under development. This gound rule in certain instances resulted in some mission performance loss. However, it was felt to be desirable in a study the main purpose of which was to establish the feasibility of a new technology for space missions.

Mission Analysis

This mission analysis study has considered the following three missions: 1) a 600-day asteroid belt probe (to 4 a.u.), 2) a solar probe (to 0.3 a.u.), and 3) a 25° out-of-ecliptic probe. It was desired to find a low-thrust spacecraft design that, when used in conjunction with an Atlas/Centaur launch vehicle, would provide the capability to perform these three missions.

The object of the study was to find a single propulsion system and spacecraft design capable of efficiently performing all three of the aforementioned missions. This objective implies that the final design will not be optimum for any one of the three missions, if optimum is used to mean maximizing the performance for that mission. In actuality, the optimum will be that spacecraft design and propulsion system that make the most satisfactory compromise between the somewhat conflicting requirements of the three missions.

Mission analysis studies were initiated by assuming certain characteristics of the spacecraft and propulsion system.

1) A rollout solar panel with a nominal specific mass of 15 kg/kw was assumed. The power available from the solar cells is presumed to decrease as a function of time due to radiation damage. This damage is presumed to lead to a 15% degradation in power available, and an actual solar panel specific mass of 17.65 kg/kw (15/0.85) has been assumed.[8]

2) Propulsion system efficiency, injected mass, and relative power were computed from the data of Table 1 (quadratically interpolated). It should be noted that the final mission profiles do not utilize the propulsion system inside 0.6 a.u., outside 2.7 a.u., or at relative power levels greater than 1. Performance is not sensitive to the date of launch for the missions considered.

Table 1 Trajectory input data

Specific impulse	Propulsion system efficiency	Heliocentric radius, a.u.	Relative power	C_3	Injected mass, kg
2000.	0.5075	0.60	1.53	0.	1200.
2250.	0.5482	0.62	1.52	10.	880.
2500.	0.5815	0.64	1.50	20.	600.
2750.	0.609	0.66	1.48		
3000.	0.6316	0.70	1.43		
3250.	0.6504	0.75	1.37		
3750.	0.6795	0.85	1.2		
4000.	0.6907	1.	1.		
4250.	0.7003	1.25	0.742		
4750.	0.7158	1.5	0.567		
5000.	0.722	2.	0.361		
		2.5	0.230		
		3.	0.165		
		4.	0.103		
		5.	0.0722		

Presented as Paper 69-252 at the AIAA 7th Electric Propulsion Conference, Williamsburg, Va., March 3–5, 1969; submitted April 8, 1969; revision received August 4, 1969.

* Manager, Ion Physics Dept., Hughes Research Laboratory, Malibu, Calif. Member AIAA.

† Senior Staff Engineer, Hughes Space Systems Division; now Electric Propulsion Program Manager, North American-Rockwell Corp., Downey, Calif.

‡ Senior Staff Engineer, Hughes Space-Systems Division, El Segundo, Calif.

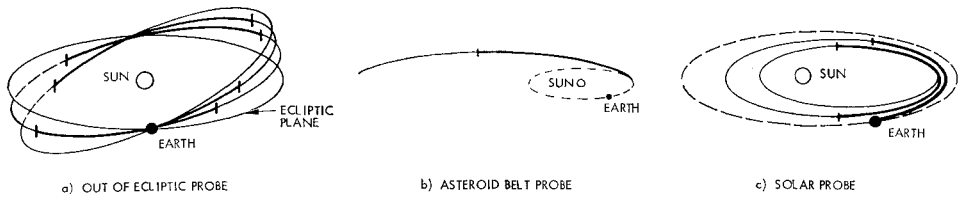

Fig. 1 Schematic trajectory profiles.

3) The propulsion system was presumed to include five power conditioning panels and six thruster modules.

4) A previous design study[2] indicated the over-all system advantages of a spacecraft design that does not permit a relative change between the thrust axis and the plane of the solar panels, and this configuration was chosen. Thrust vector orientations are obtained by rotating the entire vehicle, these excursions being limited by the performance loss resulting from the loss in spacecraft power when the solar panels are not held normal to the sun vehicle line. The thrust vector orientation for the asteroid belt probe mission was allowed to vary as much as 25° from normal to the sun line. (Note: the influence of this design choice was investigated and the results shown herein.)

5) For the asteroid belt probe, five engines were assumed to be operating initially. For the solar probe, five engines were assumed to be operating on the first thrusting phase and four engines on the second. For the out-of-ecliptic probe, five engines were presumed to be operating on the first two thrust phases and four engines on the last two. This reduction in capability for the solar probe and the out-of-ecliptic probe missions has been assumed in order to increase the probability of success on these two missions. (Note: on the basis of the study results, a different thrust time profile has been selected for the out-of-ecliptic probe.)

The performance map that was first developed is shown in Fig. 2. Net weight is total spacecraft weight less the weight of electric propulsion system (fuel, solar panel, thrusters, etc.). Curves for the asteroid belt probe and solar probe are optimized in those variables that contribute most significantly to performance (specific impulse, hyperbolic excess velocity direction and magnitude, and thrust time profile). The out-of-ecliptic probe has not been optimized. The optimum for this mission would provide greater performance capability but would require values of specific impulse which are higher than those shown. Since a common vehicle and propulsion system to perform the three missions was being sought, introducing a further mismatch in design requirements between the out-of-ecliptic and the other missions was not deemed worthwhile.

The performance capability of the solar probe if adequate thrusters and power conditioning panels are included in the design to utilize all of the power available from the solar panels is indicated. The weight of the extra propulsion system modules (five additional thrusters, two of which are standbys, and three additional power conditioning panels) has been included. However, the increase in spacecraft structural weight required to include these extra subsystems in the design has not been included and would reduce the performance advantage indicated. This concept of adapting the design to utilize all of the solar panel power was rejected for the following reasons: 1) Maximum performance advantage does not exceed about 5% in net weight; 2) theoretical performance advantages can be obtained only by introducing packaging problems that make the spacecraft design impractical, if not impossible; and 3) use of all available power along the trajectory would introduce an obvious mismatch in the number of thruster and power conditioning units required by the other missions.

It would be possible to introduce a compromise thrust time profile between the values assumed in the curves indicated, but this would merely serve to reduce the seriousness of objections 2 and 3. Furthermore, it seems unlikely that substantial performance benefits could be obtained.

The final curve shows the effects of utilizing the foldout solar panel for the asteroid belt probe. As expected, the optimum occurs at lower values of power and specific impulse rather than for the lighter weight rollout array. The performance change is almost totally represented by the difference in the solar panel weights themselves.

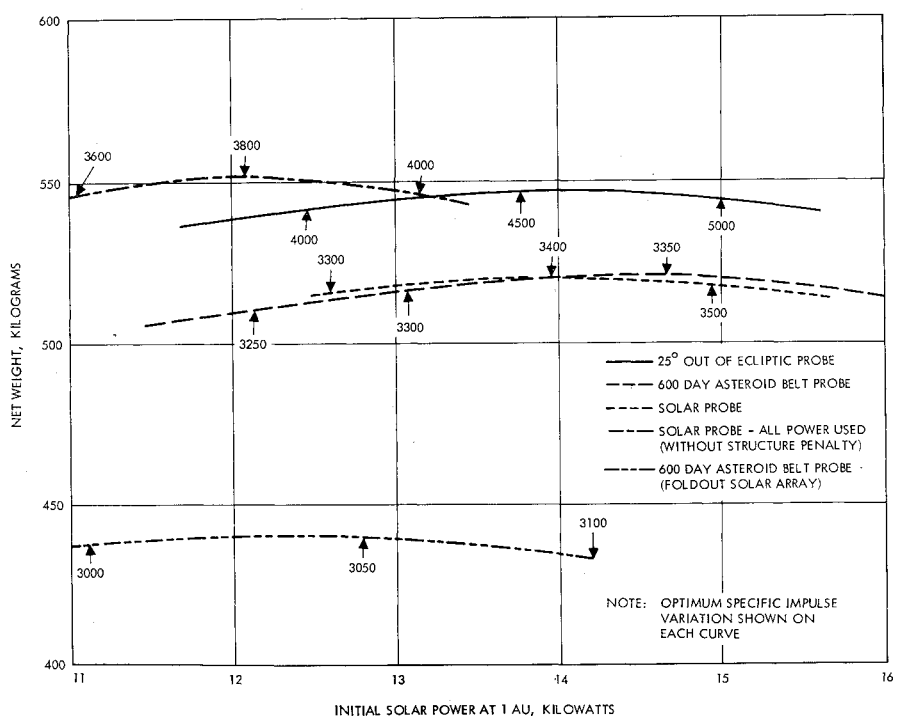

Fig. 2 Mission optimization.

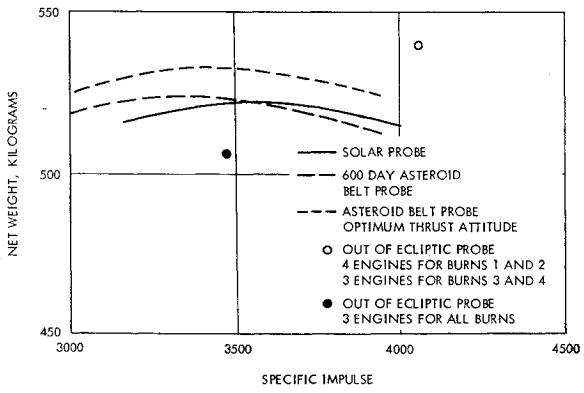

Fig. 3 Specific impulse optimization at fixed thruster module power.

Figure 2 indicates that the design power level should be approximately 14 kw at 1 a.u. This value was assumed for the second phase of the mission studies.

Figure 3 shows the results of a more detailed optimization of the three missions, assuming an initial power level of 14 kw. The curves for the solar probe and the asteroid belt probe missions are straightforwardly obtained. The third curve was generated assuming optimum values for thrust attitude on the asteroid belt probe. Introducing this additional flexibility provides a theoretical performance advantage of about 3% in net weight, but the complications in spacecraft design required to achieve this less restricted thrust attitude time history incur a weight penalty that has not been included in the curves. It is entirely possible that this increased spacecraft weight would eliminate completely the small theoretical performance advantage. The influence of a design requirement for this more general thrust attitude orientation capability is discussed in the spacecraft design section.

It is indicated in Fig. 2 that the high specific impulses required for the out-of-ecliptic probe mission introduce a mismatch with the propulsion systems required for the other two missions. Therefore, modified thrust time profiles were used for the out-of-ecliptic probe. On one profile four engine modules are utilized for the first two thrust phases and three engine modules are utilized for the third and fourth thrust phases; on the other profile three engine modules are used for all thrust phases. The trajectories represented by these thrusting profiles have propulsion subsystems that are identical with those used on the other curves (i.e., five power conditioning panels and six thruster modules). However, the solar panel carried has been reduced by 20 and 40%, respectively. These modifications can be very simply incorporated without changing the basic 14.0 kw spacecraft design. These reduced thrust profiles permit a mission reliability commensurate with the other missions despite the increased thrusting time (530 days vs 320 for the asteroid belt probe and 240 for the solar probe).

On the basis of the results discussed earlier, the propulsion system design has been chosen to operate at a specific impulse of 3500 sec and to contain five power conditioning panels with an input power of 2.8 kw each and six thruster modules with an input power of 2.6 kw each. The asteroid belt probe and the solar probe will utilize a rollout solar panel with (degraded) power of 14 kw at 1 a.u. The out-of-ecliptic probe mission will utilize a rollout solar panel with (degraded) power of 8.4 kw at 1 a.u. The values of C_3 are 3.03, 2.22, and 0.78 $(km/sec)^2$ for the asteroid belt probe, solar probe, and out-of-ecliptic probe, respectively.

Multimission Spacecraft Design

A feasible solar electric spacecraft design capable of performing three different missions (e.g., asteroid belt probe, solar probe, and out-of-ecliptic probe) is shown in Fig. 4. Based on the results of the mission analyses, a design point was selected (power level and specific impulse) that permitted the use of electric propulsion system components presently under development at Hughes Aircraft Company. A single spacecraft concept was then designed around the selected propulsion system. With only very minor modifications, this spacecraft configuration is able to perform any of the multimissions studied. The Atlas (SLV-3C)/Centaur with a standard OAO shroud was the only launch vehicle considered.

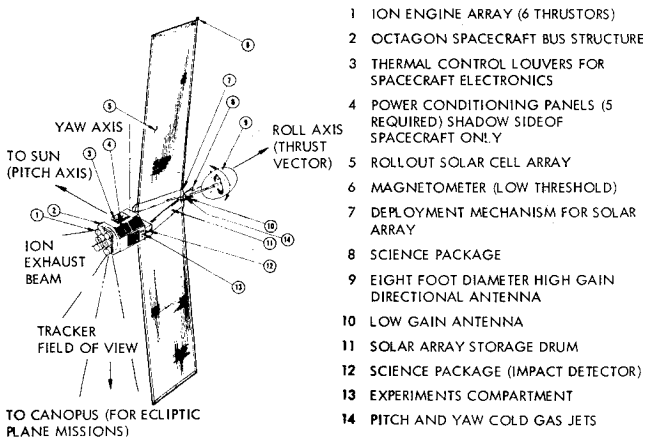

Fig. 4 SEP multimission spacecraft, deployed configuration.

The spacecraft design was limited to consider only the following features:

1) Rollout-type solar cell panels (FISCA—flexible integrated solar cell arrays) were chosen because of their lower specific weight (15 kg/kw) in comparison to large area folding modular arrays (21 kg/kw). Another advantage in selecting the rollout arrays is that they require less stowage volume than foldouts. Figure 5 shows that for the power levels considered (approximately 7 kw per rollout assembly), foldout arrays require about twice the stowage volume.

2) The deployed solar panels are fixed with respect to the spacecraft. In other words, no provisions were incorporated to change the orientation of the thrust vector with respect to the plane of the solar array. In the preceding section on trajectory analyses, the negligible performance benefits in being able to optimally swing the thrust vector were pointed out. The spacecraft design implications of providing this feature will be discussed later in this section.

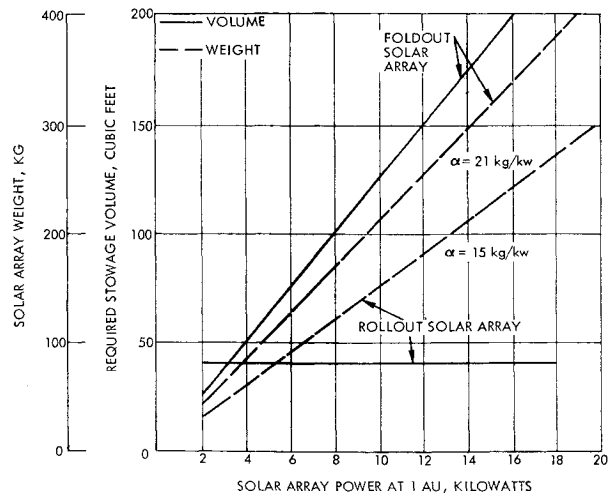

Fig. 5 Required stowage volume and weight vs power at 1 a.u. for rollout and foldout solar cell arrays.

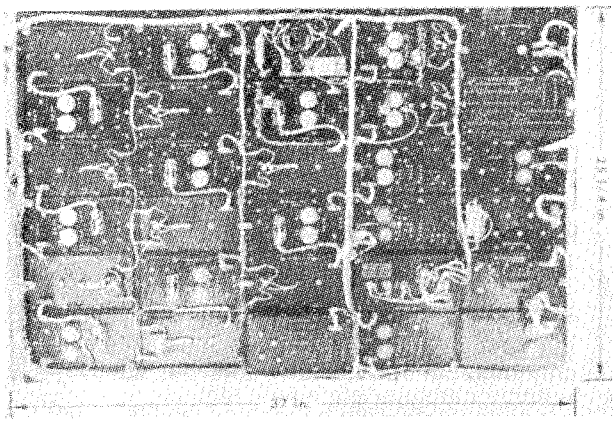

Fig. 6 2.5 kw power conditioning panel.

3) The propulsion system consists of a thruster array of six engines, five power conditioning and control subsystems, and a single spherical propellant tank with a liquid mercury capacity of 910 lb. Because of the wide variation in the trajectory characteristics of the three missions studied, the programing of the thruster modules, the reliability of the propulsion system, and the amount of propellant will vary.

It has been clearly demonstrated in previous studies (Ref. 3) that the capability of modularizing the three major subsystems (i.e., thruster and feed, power conditioning and control, and reservoir) affords relatively high system reliability at minimum weight penalties. Following these general guidelines, the propulsion system design considered in this study is based on a 2.6 kw thruster module of the type shown in Fig. 7 (Ref. 5) and a modularized power conditioning and control subsystem such as that presented in Fig. 6. The thruster[5] shown is presently undergoing integration and life-testing at JPL. Thus, by using these basic building blocks, it is possible to design a modularized propulsion system that is within the capability of present technology.

(It should be noted that Ref. 6 describes a propulsion system design methodology which for a given application results in an optimum system design based on a weight-reliability-power matching criterion. Furthermore, Ref. 7 discusses the iterative procedure required to properly interrelate the trajectory analysis and propulsion system design analysis. Using the analytical procedures presented in these two references, an optimization of both low-thrust trajectory and propulsion system design can be accomplished. With the availability of these analytical tools, higher performance trajectories and propulsion systems can be expected, thereby increasing the payload capabilities of SEP spacecraft presented in this paper.)

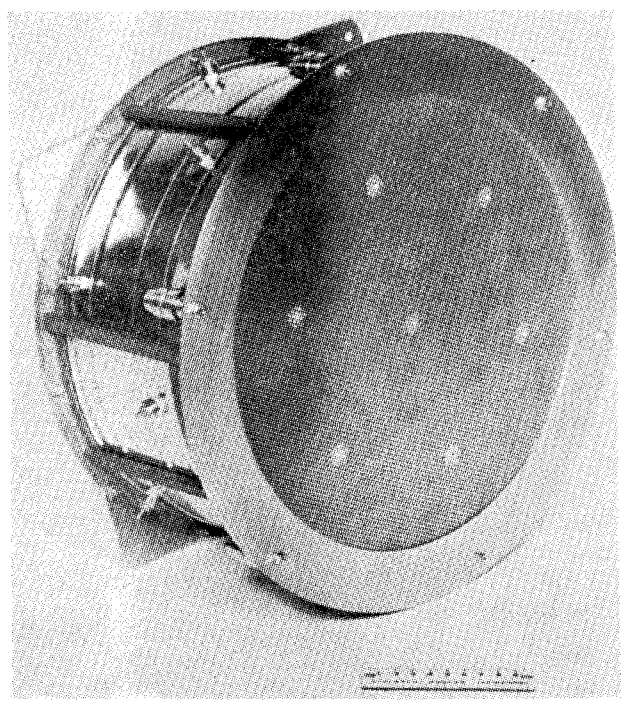

Fig. 7 30 cm mercury bombardment thruster.

Table 2 Weight summaries for SEP multimission spacecraft (ATLAS SLV-3C/launch vehicle)

Items	Missions: Asteroid belt probe	Solar probe	Out-of-ecliptic probe
Mission Payload	230	229	256
Weight available for science equipment	125	124	151
Telecommunications and data handling	82	82	82
Power (batteries)	23	23	23
Solar electric propulsion system	367	367	268
Solar array rollout (33 lb/kw)[a]	247	247	148
Power conditioning (5 at 22 lb each)	50	50	50
Thrusters (6 at 8 lb each)	22	22	22
Reservoir	9	9	9
Auxiliary equipment (cabling, switching circuitry, piping, structure, mechanisms, and power logic)	39	39	39
Propellant (liquid mercury)	250	277	414
Structure	82	82	82
Guidance and control	55	55	55
Thermal control	23	23	13
Electric harness	11	11	11
Contingencies (10% of injected weight, less propellant)	85	85	76
Total spacecraft injected weight, kg	1103	1129	1175

[a] Includes solar power to spacecraft subsystems and science.

Spacecraft Configuration

The SEP multimission spacecraft in the stowed configuration is depicted in Fig. 8. The basic spacecraft body (80 in. long and 72 in. wide) is an octagonal structure that is attached to a conical Centaur adapter (separation plane) at one end. The body structure is shown in more detail in Fig. 9. The electric engine array composed of six thrusters is mounted to this aft end of the spacecraft and is contained within the adapter during launch. Each face of the octagonal structure is 30 in. wide and the five power conditioning panels are attached to the three faces that are on the shadow side of the vehicle. A conical structure within the octagon serves

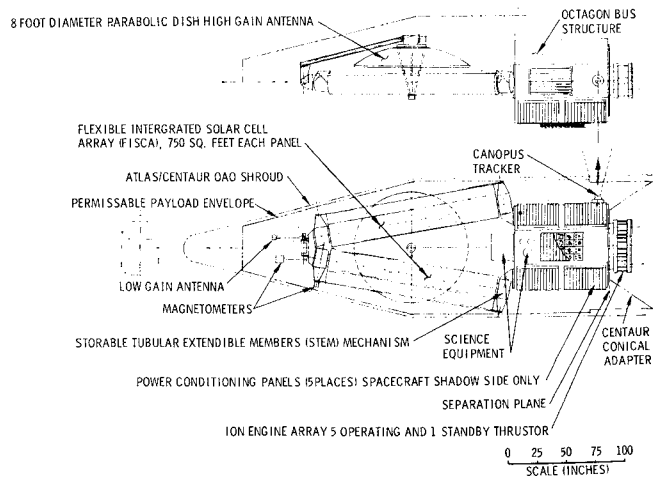

Fig. 8 SEP multimission spacecraft general arrangement, stowed configuration.

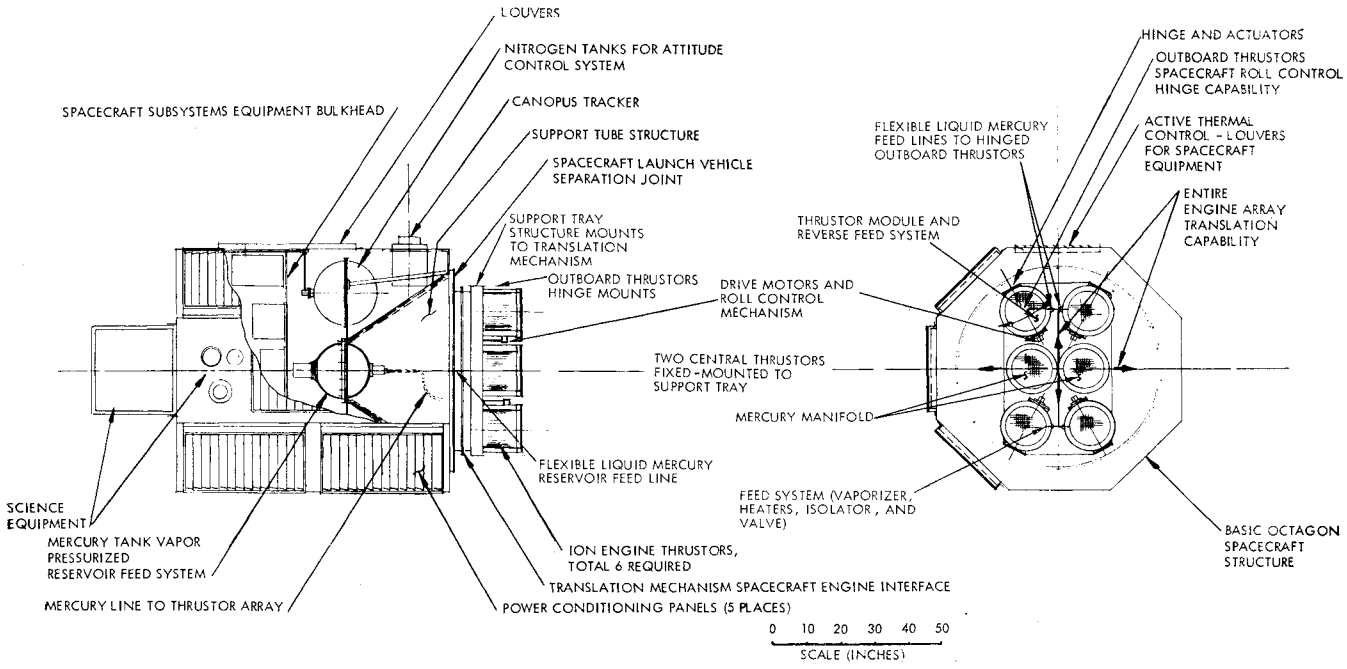

Fig. 9 SEP multimission spacecraft body arrangement.

to centrally support the single liquid mercury reservoir. The launch loads are transmitted directly to the spacecraft adapter interface. Four spherical cold gas tanks for attitude correction are peripherally mounted within the central portion of the spacecraft. The jets for pitch or yaw maneuvers are placed on the forward tip of the spacecraft to maximize their moment arm. The roll jets are mounted on the octagon. In addition to sun sensors, a star tracker is located at the rear end of the octagon. For missions whose trajectories are primarily in the ecliptic plane, this arrangement affords the Canopus tracker an adequate field-of-view. For the out-of-ecliptic mission, a different arrangement must be considered. Since the spacecraft's attitude is alternated during the mission, the consideration of using a star in the northern celestial sphere in addition to Canopus may be desirable. For the out-of-ecliptic missions, the star trackers could be mounted to view diametrically opposite the thruster's exhaust beam at the upper end of the spacecraft. Preceding each of the four thrusting phases, acquisition and lock-on of the appropriate reference star would be made. These maneuvers would be accomplished by a three axis cold gas system that would pitch the spacecraft about the sunprobe line. An alternate method would require gimballing the tracker (180° rotation) to enable it to be oriented toward Canopus during opposite thrusting phases. This method does not seem as attractive because of the additional mechanization and potential masking of the field-of-view by the engine's exhaust beam.

At the forward end of the octagon, an equipment bulkhead is provided for all the spacecraft subsystem electronics. Two of the eight octagon bays are devoted to housing science equipment. The enclosed volume is actively thermally controlled by the use of radiation control louvers. Science packages may also be mounted and field-of-view oriented on the forward closure of the octagon.

Two rollout solar cell arrays, each capable of providing 7 kw at 1 a.u., are mounted to the forward end of the structure. Each of the rolled up substrates is deployed by the use of two storable tubular extendible member (STEM) mechanisms. The panels are extended outward from the spacecraft and are canted forward to make optimum use of the conical portion of the OAO shroud and to provide adequate field-of-view clearance for the Canopus tracker.

This configuration permits the use of a large (8-ft diam) high gain antenna. In the stowed position the antenna mast is folded back to fit within the shroud. The antenna pointing mechanism, which has two degrees of freedom, maintains proper communication attitude through the mission. For the out-of-ecliptic mission, where the earth-probe distances remain relatively close, consideration should be given to using only a low gain antenna. Sensors sensitive to spacecraft generated environments, such as magnetometers and electric field meters, are placed on the extreme forward tip of the spacecraft.

A representative weight summary is shown in Table 2 for the three missions considered. The injected weights vary for the three missions, each of which requires unique performance levels by the launch vehicle (different C_3 values). The basic variations in weight summaries for each mission can be seen primarily in three items: liquid mercury propellant, solar arrays, and science equipment. A 10% contingency based on the injected weight has been included. A significant weight allocation for experiments is available on all missions as seen from the spacecraft weight summaries in Table 2.

The ion engine array, composed of six nominal 30 cm (2.6 kw) thruster modules, is shown in Fig. 9. The two center thrusters are rigidly attached to the engine support platform. The other four thrusters are hinged to enable using them for roll axis correction torques. Due to the unsymmetrical nature of "on" thruster operations for 5 and 3 thrusters firing, the entire engine platform is intended to be translated both vertically and horizontally to maintain resultant thrust vector and spacecraft center of mass alignment. The translation mechanism also provides attitude control capability in pitch and yaw during thrusting phases. Disturbances due to solar pressure torques, which are unavoidable due to the center of pressure-center of mass offset caused by the canted solar cell panels, can be cancelled by slightly biasing the thrust vector off the center of gravity. A number of mechanical translation schemes could be applied which would all require control logic circuitry for disturbance rate sensing and compensation by moving the engine array.

Design complications arise if variable thrust vector attitude is considered. As indicated previously (Fig. 3), only a 15 kg increase in net weight results for the asteroid belt probe mission if the thrust vector attitude is optimized (approximately

a 60° sweep). Accepting a constant attitude system, while allowing minor off-normal solar panel orientation during thrusting, negligibly degrades mission performance. Conceptual designs have been formulated incorporating 360° rotational capability between the plane of the solar cell panels and the basic spacecraft body, but failure of the rotational system will abort the mission. To maintain center of mass stability, the mercury reservoir should be at the vehicle's center of gravity. This implies that the reservoir is the central part of the rotation device between the solar panels and the basic structure. Even if such a mechanical system could be designed well within the 15 kg margin, the reliability factors of such a system do not merit its consideration for the multimission spacecraft design.

Conclusion

Based on the results of low-thrust trajectory analyses for three unique missions (asteroid belt probe, solar probe, and out-of-ecliptic probe), a single set of propulsion system parameters was found that permitted use of a common solar electric propulsion system for multimission SEP spacecraft design. The components in the selected propulsion system design are representative of the present ion propulsion system technology. A single, uncomplicated spacecraft design concept was formulated that has the capability of carrying a large complement of science equipment (approximately 600 lb) for any of the three missions studied. In summary, although optimum performance for each mission is not achieved by a single spacecraft design, only minor modifications to the spacecraft are necessary to efficiently perform any one of the three missions studied. Thus, such a spacecraft appears extremely attractive for near term solar electric propulsion missions using an Atlas (SLV-3C)/Centaur launch vehicle.

References

[1] Meissinger, H. F., Park, R. A., and Hunter, H. M., "A 3 KW Solar-Electric Spacecraft for Multiple Interplanetary Missions," AIAA Paper 67-711, Colorado Springs, Colo., 1967.

[2] "Solar Powered Electric Propulsion Program," Program Summary Report, SSD 60374R, Dec. 1966, Hughes Aircraft Co.

[3] Molitor J. H. et al., "Design of a Solar-Electric Propulsion System for Interplanetary Spacecraft," *Journal of Spacecraft and Rockets*, Vol. 4, No. 2, Feb. 1967, pp. 176–182.

[4] King, H. T., Poeschel, R. L., and Ward, J. W., "2½ kW Low Specific Impulse, Hollow-Cathode Mercury Thruster," AIAA Paper 69-300, Williamsburg, Va., 1969.

[5] Pawlik, E. V., Macie, T. W., and Ferrera, J. D., "Electric Propulsion System Performance Evaluation," AIAA Paper 69-236, Williamsburg, Va., 1969.

[6] Seliger, R. L., Russell, K. J., and Molitor, J. H., "Electric Propulsion Design Optimization Methodology," AIAA Paper 69-254, Williamsburg, Va., 1969.

[7] MacPherson, D., "Mission Analysis Technology," *7th Electric Propulsion Conference*, Vol. 4, AIAA, New York, 1969.

[8] Smith, A. H., Cohn, E. M., and Maxwell, P. T., "Solar Cell Electrochemical Power Supplies—10 watts to 50 kw," Preprint IX E.2, June 1969, American Astronautical Society and DRS.

NOVEMBER 1969 J. SPACECRAFT VOL. 6, NO. 11

Optimal Estimation of Rotation-Coupled Flexural Oscillations

JAMES L. FARRELL,* JAMES K. NEWTON,† JAMES A. MILLER,‡ AND ELIEZER N. SOLOMON§
Westinghouse Defense and Space Center, Baltimore, Md.

The Radio Astronomy Explorer satellite, presently orbiting the Earth and holding an accurate local orientation by four 750-ft booms, experiences significant static and dynamic elastic deformations in orbit. The gravity-gradient librations, which actually are coupled to the flexure at these boom lengths, are observable at close intervals while the boom tips are monitored only when the satellite is within range of certain TV stations. An iterative weighted least-squares estimation program has been developed, in which a time history for the state (attitude, damper displacement, and elastic deformation) is reconstructed, using all pertinent data available. A companion program, capable of generating hypothetical data corrupted by additive Gaussian noise, has been used to demonstrate successful reconstruction, augmented by instrument bias detection and improved determination of certain system parameters. Linearized ensemble statistics have been generated, to predict performance under various conditions.

Nomenclature¶

a_i = solar heat absorptivity of ith antenna ($1 \leqslant i \leqslant 4$)
$\mathbf{A}_i$ = unit vector along sensitive axis of ith magnetometer ($1 \leqslant i \leqslant 3$)
$\mathbf{b}$ = 3×1 vector of magnetometer bias errors
$[B_i]$ = canonical dynamic coefficient matrix during ith interval
$[C']$ = orthogonal transformation from hub principal axes to local coordinates
d = boom diameter
$[d],[m]$ = coefficient matrices for first and second time derivatives, respectively, of generalized coordinates in equations of motion
e = linear thermal expansion coefficient for booms
$\boldsymbol{\mathcal{E}}$ = 5×1 vector of satellite parameters, a_1–a_4; EI
E = boom modulus of elasticity
EI = boom flexural rigidity
$[\mathcal{G}]$ = 24×5 matrix, $\partial\dot{\mathbf{X}}/\partial\boldsymbol{\mathcal{E}}$
$[G_{m,i-1}]$ = integrated effect of variations in $\boldsymbol{\mathcal{E}}$, from beginning of ith interval to time (t_m)
$[H_m],[\mathfrak{M}_m]$ = matrix of partial derivatives of observables with respect to current state and with respect to initial state, respectively

Received November 18, 1968; revision received August 18, 1969. Contract NAS5-9753-20, Goddard Space Flight Center.

* Fellow Engineer, Control Data Systems Section. Associate Fellow AIAA.

† Engineer, Control Data Systems Section. Member AIAA.

‡ Supervisory Engineer, Digital Analysis and Control Section.

§ Associate Engineer, Digital Analysis and Control Section.

¶ Mks units; all angles in radians.